

## Pitting Corrosion Inhibition of Some Copper Alloys in Neutral Solutions by Straight Chain Carboxylates

S.S. Mahmoud,\* M.M. Ahmed, A.H. Marie and R.A. El-Kasaby

*Chemistry Department, University College of Girls for Arts, Science and Education,  
Ain shams University, Heliopolis, Cairo, Egypt*

Received 10 January 2007; accepted 20 July 2007

---

### Abstract

Electrochemical methods were used to investigate the abilities of the homologous straight chain monocarboxylates ( $C_nH_{2n+1}COO^-$ ,  $n=1-13$ ) to inhibit the pitting corrosion of two types of copper alloys in aerated, saline and near neutral aqueous solutions. The copper alloys were alloy (I) (Cu + 4.47% Fe) and alloy (II) (Cu + 10.67% Al + 5.02% Fe). It was found that these were susceptible to pitting corrosion in NaCl solutions, with increase of  $Cl^-$  ions concentration. Alloy (II) was more susceptible to pitting corrosion than alloy (I). The performance of monocarboxylates was shown to be critically dependent upon their chain length. The range of chain lengths producing optimal inhibition was ( $6 \leq n \leq 10$ ). These carboxylates showed abrupt decreases in inhibitor ability outside the optimal range. The dramatic variations in inhibition efficiencies probably resulted from competing reactions such as adsorption, solubility and micelle formation.

**Keywords:** adsorption, copper alloys, pitting corrosion, monocarboxylates, polarization, galvanic current, inhibition.

---

### Introduction

A lot of work has been done on the use of organic molecules to inhibit corrosion of metals in contact with aqueous solutions [1-5]. The majority of such studies have been carried out in aggressive, usually acidic, solutions. However, it is known that the chemical form of organic inhibitors often depends on pH.

This in turn, may alter their adsorbability, solubility, or complexing capability dramatically. Corrosion mechanisms also may differ significantly between acidic and neutral aqueous solutions because of the presence and/or differing nature of metal oxide / hydroxide films at higher pH values [6-8]. For these reasons, it can

---

\* Corresponding author. E-mail address: drsohairr@hotmail.com

be misleading to draw conclusions about likely inhibitor effectiveness in neutral solutions on the basis of data obtained in acidic solutions [9].

In many practical situations, such as automotive and other heat exchange systems, steam boilers, etc., solution conditions are neutral. Furthermore, the common practice of using normal tap water as the coolant or for make up, invariably introduces chloride ions ( $\text{Cl}^-$ ), which can have a pronounced effect corrosion behaviour and/or pitting corrosion.

There is a clear need for detailed information on the behaviour of organic inhibitors in neutral solutions in the presence of chloride ions. Yet despite the vast literature on organic corrosion inhibitors, relatively few systematic studies have been made, particularly in neutral solutions [1-9]. Among various types of available organic compounds, straight chain aliphatic carboxylates show good inhibition characteristics towards a number of metals [10]. In addition, carboxylates are environmentally benign, as they have low toxicities and are really biodegradable.

The objective of the present work was to investigate the ability of straight chain aliphatic carboxylates to inhibit the pitting corrosion of some copper alloys in sodium chloride solutions. These alloys were chosen because they are the common metallic components of most heat-exchange systems, especially modern automotive cooling systems. The compounds studied were the monocarboxylates ( $\text{C}_n\text{H}_{2n+1}\text{COO}^-$  from  $n=1$  up to  $n=13$ ). All measurements were made in aerated, saline, weakly buffered, and near-neutral aqueous solutions that were reasonably representative of mains or tap water commonly used in practical heat-exchange situations.

## **Experimental**

In this investigation two types of copper alloys were used having the composition: alloy I (Cu + 4.47% Fe), alloy II (Cu + 10.67% Al + 5.02% Fe). The electrodes were jammed in a small copper mould with about 30 cm wire tail which was fixed in a glass tube with Araldite epoxy adhesive resin. The apparent cross sectional area of all electrodes were  $1.54 \text{ cm}^2$ .

Prior to each experiment the test electrodes were polished mechanically using emery papers of different grades to a final 1200 grit. After this the electrodes were degreased with acetone and washed with deionized water. Complete wetting of the surface was taken as an indication of its cleanliness. The electrodes were then immersed immediately in the test solution. The test solution was aerated by passing a gentle stream of air, presaturated with test solution to minimize evaporative losses, through the test solution via capillary bubbles.

NaCl solutions used in this work were prepared from Analar grade reagents by appropriate dilution with deionized water. The organic additives were the monocarboxylates ( $\text{C}_n\text{H}_{2n+1}\text{COO}^-$  up to  $n=13$ ). These inhibitors were commercial laboratory-grade reagents used without further purification. Where necessary, the pH of each test solution was adjusted to  $8.4 \pm 0.1$  by addition of a small volume of 1.0 M sodium hydroxide or 1.0 M perchloric acid. The solution pH was measured using a combined glass electrode and a Radiometer Model 85 ion analyzer.

The pitting potentials were determined from the potentiodynamic anodic polarization measurements at a scanning rate of 1 mV/sec, using a Wenking Potentioscan type POS 73. The current density-potential curves were recorded on an X-Y recorder type PL-3. The potentials were measured relative to a saturated calomel electrode (SCE). Also, the galvanic current as a function of time was recorded. A platinum electrode was used as a counter electrode. The current was measured by means of a multimeter (Keithley, Model 130A, USA). All measurements were carried out at 25 °C.

### Results and discussion

Figs. 1 and 2 show the potentiodynamic anodic polarization curves for alloys (I, II), respectively, in NaCl solutions of different concentrations (ranged from 0.01-1.0 M) at a sweep rate of 1 mV/sec. It can be seen from the polarization curves that the flowing currents increase suddenly at definite potentials, which are called pitting potentials ( $E_{pit}$ ), in the passive region. The values of  $E_{pit}$  greatly depend on the concentration of NaCl solution. This increase in current is due to the breakdown of passivity and initiation of pitting corrosion. The different values of  $E_{pit}$  for the alloys I and II in different NaCl solutions are listed in Table 1.

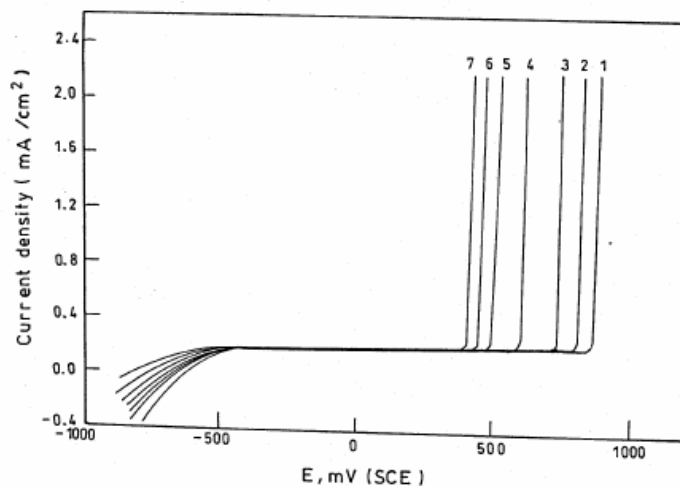


**Figure 1.** Potentiodynamic anodic polarization curves for alloy (I) in NaCl solutions of different concentrations: 1- 0.01, 2- 0.05, 3- 0.1, 4- 0.25, 5- 0.5, 6- 0.75, 7- 1.0 M.

**Table 1.** Potentiodynamic measurements for alloys I and II in different concentrations of NaCl solutions at 25 °C.

Concentration (M)	$E_{pit}$ (mV)	
	alloy I	alloy II
0.01	850	800
0.05	800	725
0.1	730	650
0.25	600	500
0.5	500	400
0.75	430	350
1.0	400	290

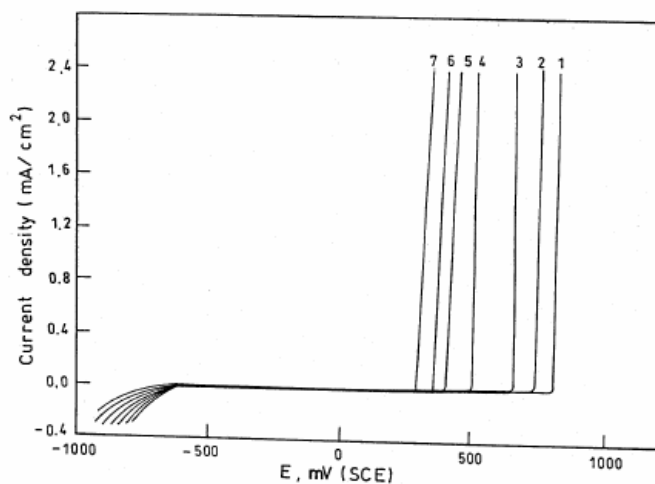


**Figure 2.** Potentiodynamic anodic polarization curves for alloy (II) in NaCl solutions of different concentrations: 1- 0.01, 2- 0.05, 3- 0.1, 4- 0.25, 5- 0.5, 6- 0.75, 7- 1.0 M.

The dependence of the pitting potential,  $E_{pit}$ , on the  $Cl^-$  ions concentration is shown in Fig. 3. This figure represents the variation of the pitting potential,  $E_{pit}$ , with the logarithm of the molar concentration of  $Cl^-$  ions for alloys (I, II).

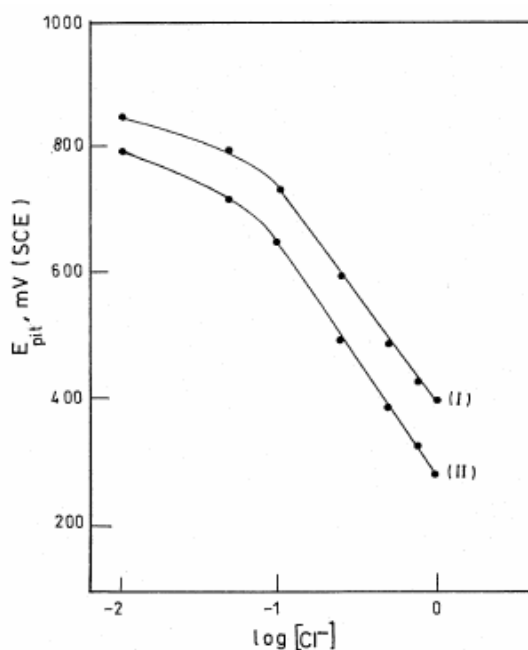


**Figure 3.** Variation of  $E_{pit}$  with logarithm of the molar concentration of chloride ions for alloys (I, II).

Most investigation carried out on the pitting corrosion revealed a straight line relationship between  $E_{pit}$  and  $\log C_{Cl^-}$  in a form like [11-13]:

$$E_{pit} = a_1 - b_1 \log C_{Cl^-} \quad (1)$$

where  $a_1$  and  $b_1$  are constants, which depend on the nature of the metal and type of the aggressive anion. However, in this case the plots of Fig. 3 are of sigmoidal

nature in which equation (I) is obeyed at concentration of chloride ions higher than 0.05 M. At lower concentration the pitting corrosion,  $E_{\text{pit}}$ , changed only slightly in the negative direction (less noble) as the concentration of chloride ions was increased. In this case, it can be concluded that these low concentrations of chloride are not sufficient to destroy completely the passivating film formed on the metallic surface. Also, the pits formed are not completely active and may undergo repassivation [3-15]. At higher concentrations of chloride ions the pits formed are assumed to be of the limiting active type. But in the presence of still higher concentrations of chloride ions, the pits formed are assumed to be non passivable active ones. These concentrations of the chloride ions are sufficient to cause continuous propagation of the pits already formed.

Also, the plots of Fig. 3 indicate that, at a given chloride concentration, the pitting corrosion,  $E_{\text{pit}}$ , for the alloy (I) is more positive than that for the alloy (II). This means that alloy (II) is more susceptible to pitting corrosion in NaCl solutions than alloy (I). This was indicated from the values of  $b_1$  for the two alloys which are equal to 330 and 360 mV/decade for alloy I and alloy II, respectively.

The effect of organic additives (1-13) in 1.0 M NaCl solution on the pitting potential,  $E_{\text{pit}}$ , of the alloys (I,II) was further investigated using the potentiodynamic anodic polarization technique. Figs. 4 and 5 show the potentiodynamic anodic polarization curves for alloys (I,II), respectively, in 1.0 M NaCl solution containing increasing concentrations ( $10^{-5}$ - $10^{-3}$  M) of the organic additive (10) at the scanning rate 1 mV/sec. Similar polarization curves were also obtained for the alloys (I,II) in the presence of other additives, but not shown.

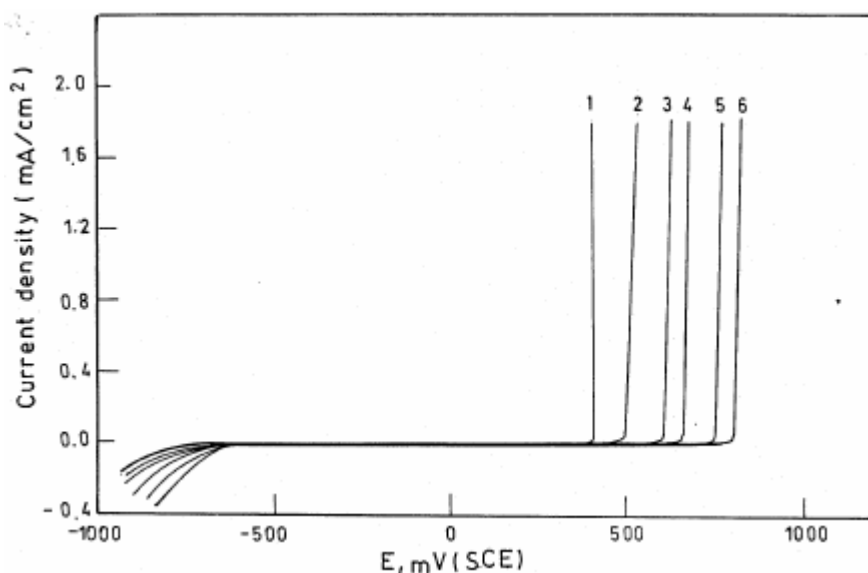


**Figure 4.** Potentiodynamic anodic polarization curves for alloy (I) in NaCl solutions in absence and presence of different concentrations of compound (10): 1- blank, 2-  $1 \times 10^{-5}$ , 3-  $5 \times 10^{-5}$ , 4-  $1 \times 10^{-4}$ , 5-  $5 \times 10^{-4}$ , 6-  $1 \times 10^{-3}$  M.

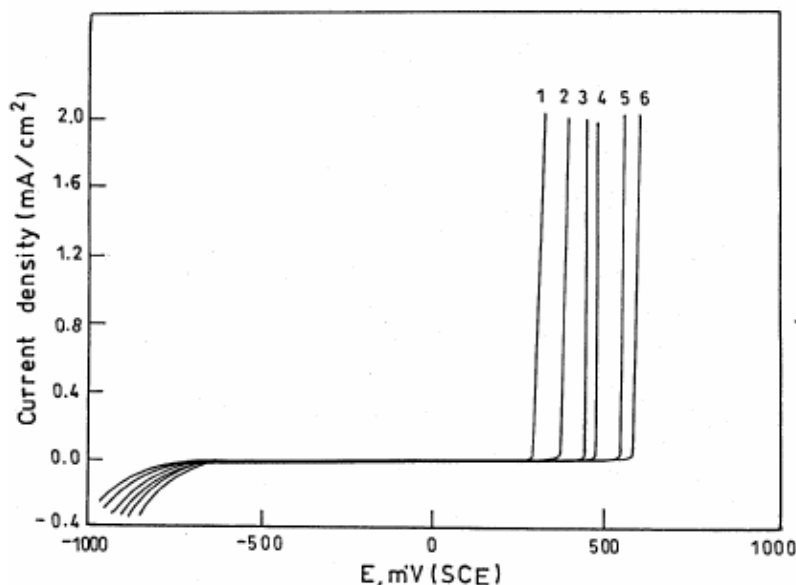
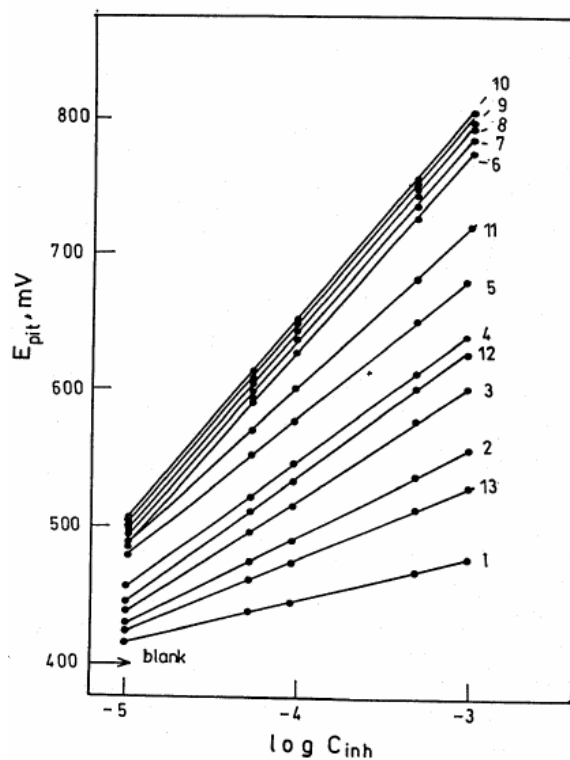


**Figure 5.** Potentiodynamic anodic polarization curves for alloy (II) in NaCl solutions in absence and presence of different concentrations of compound (10): 1- blank, 2-  $1 \times 10^{-5}$ , 3-  $5 \times 10^{-5}$ , 4-  $1 \times 10^{-4}$ , 5-  $5 \times 10^{-4}$ , 6-  $1 \times 10^{-3}$  M.

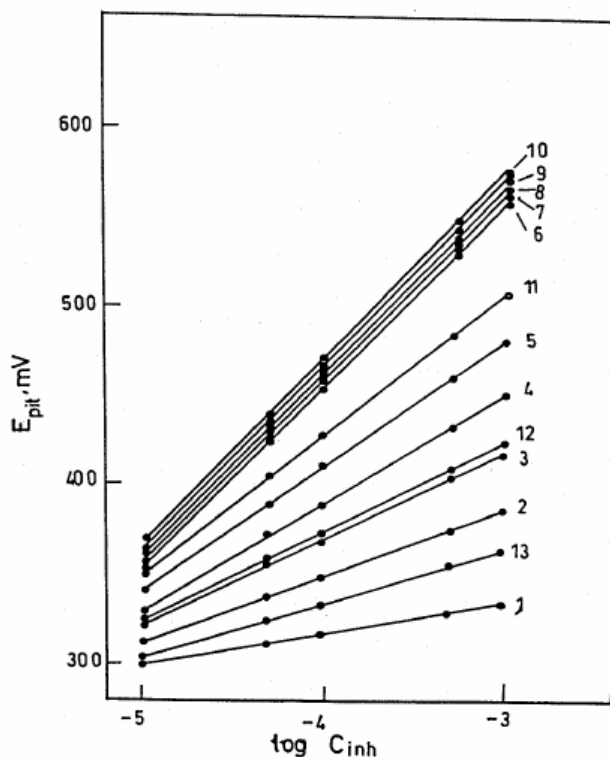
The values of  $E_{\text{pit}}$  deduced from the plots of Figs. 4 and 5 and similar ones for the alloys (I,II) immersed in 1.0 M NaCl solution in presence of different concentrations of the organic additives (1-13) are listed in tables (2-5). The dependence of the pitting potential,  $E_{\text{pit}}$ , on the concentration of organic additives is shown in Figs. 6 and 7 for alloys I and II, respectively. The obtained plots are straight lines which means that  $E_{\text{pit}}$  varies linearly with the logarithm of the molar concentration of the organic additive according to the relationship:

$$E_{\text{pit}} = a_2 + b_2 \log C_{\text{inh}} \quad (2)$$

where  $a_2$  and  $b_2$  are constants, which depend on both the type of the alloy and of the organic additives. The plots of Figs. 6 and 7 indicate that  $E_{\text{pit}}$  shifts to the noble direction in the presence of increasing concentrations of these organic additives. This means that these organic additives have inhibiting effect on the pitting corrosion of the alloys I and II in NaCl solutions. The values of  $b_2$  are deduced from the slopes of the straight lines of Figs. 6 and 7 and depicted on Fig. 8 for alloys I and II. From the plots of this figure it is evident that the value of  $b_2$  increases gradually from (1-5) and then abruptly rises and remains high up to compound (10). After this the value of  $b_2$  greatly decreases for compounds (11-13). From the plots of Fig. 8 it can be seen that the efficiency of these pitting corrosion inhibitors changes according to the order:  $1 < 2 < 3 < 4 < 5 \ll 6 \cong 7 \cong 8 \cong 9 \cong 10 > 11 > 12 > 13$ . Also, this order can be obtained from the plots of Fig. 9, where the values of  $E_{\text{pit}}$  for alloys I and II are depicted in the presence of  $10^{-3}$  M of each of the organic additive in 1.0 M NaCl solution. The obtained plots have the same feature of those of Fig. 8.



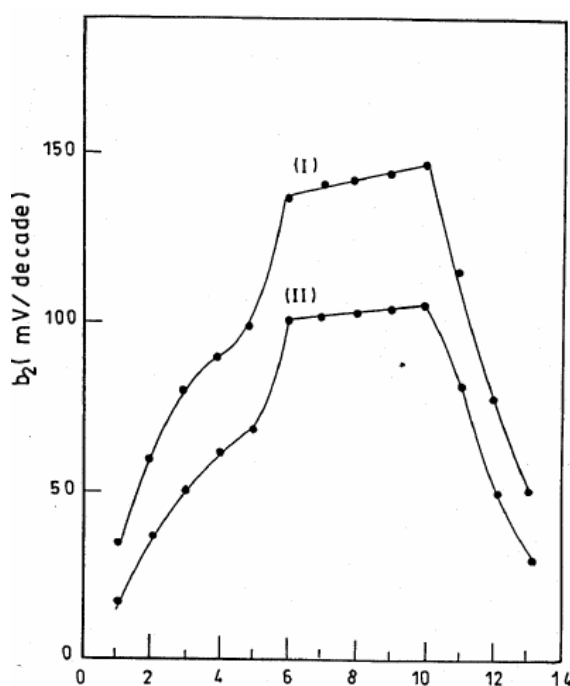
**Figure 6.** Variation of  $E_{pit}$  for alloy (I) with logarithm of the molar concentration of different organic additives (1-13).



**Figure 7.** Variation of  $E_{pit}$  for alloy (II) with logarithm of the molar concentration of different organic additives (1-13).

**Table 2.** Potentiodynamic measurements for carbon steel for alloys I and II in 1.0 M NaCl containing different concentrations of compounds (1-3), at 25 °C.

Conc. (M)	$E_{pit}$ (mV)					
	Compound 1		Compound 2		Compound 3	
	alloy I	alloy II	alloy I	alloy II	alloy I	alloy II
0.00	400	290	400	290	400	290
$1 \times 10^{-5}$	420	302	432	315	440	320
$5 \times 10^{-5}$	437	310	475	340	492	355
$1 \times 10^{-4}$	450	320	495	352	520	370
$5 \times 10^{-4}$	470	330	537	375	575	405
$1 \times 10^{-3}$	780	334	560	390	600	420

**Figure 8.** The values of  $b_2$  of the organic additives (1-13) for alloys (I,II).**Table 3.** Potentiodynamic measurements for carbon steel for alloys I and II in 1.0 M NaCl containing different concentrations of compounds (4-6), at 25 °C.

Conc. (M)	$E_{pit}$ (mV)					
	Compound 4		Compound 5		Compound 6	
	alloy I	alloy II	alloy I	alloy II	alloy I	alloy II
0.00	400	290	400	290	400	290
$1 \times 10^{-5}$	460	330	480	345	500	360
$5 \times 10^{-5}$	520	370	550	390	585	430
$1 \times 10^{-4}$	550	390	580	410	635	455
$5 \times 10^{-4}$	612	430	645	460	732	530
$1 \times 10^{-3}$	640	450	680	480	776	560

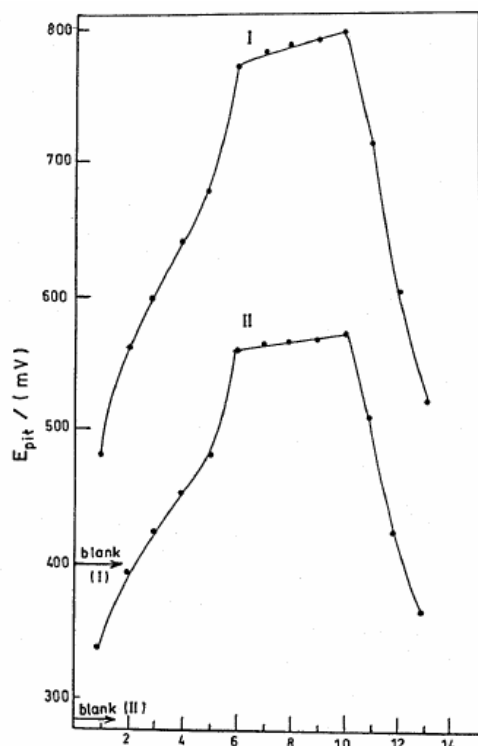


**Figure 9.**  $E_{pit}$  of  $10^{-3}$  M of organic additives (1-13) for alloys (I, II).

**Table 4.** Potentiodynamic measurements for carbon steel for alloys I and II in 1.0 M NaCl containing different concentrations of compounds (7-9), at 25 °C.

Conc. (M)	$E_{pit}$ (mV)					
	Compound 7		Compound 8		Compound 9	
	alloy I	alloy II	alloy I	alloy II	alloy I	alloy II
0.00	400	290	400	290	400	290
$1 \times 10^{-5}$	502	362	505	365	505	365
$5 \times 10^{-5}$	585	432	590	434	600	435
$1 \times 10^{-4}$	635	460	640	462	645	464
$5 \times 10^{-4}$	735	532	740	535	750	535
$1 \times 10^{-3}$	785	565	790	568	795	570

**Table 5.** Potentiodynamic measurements for carbon steel for alloys I and II in 1.0 M NaCl containing different concentrations of compounds (10-13), at 25 °C.

Conc. (M)	$E_{pit}$ (mV)							
	Compound 10		Compound 11		Compound 12		Compound 13	
	alloy I	alloy II	alloy I	alloy II	alloy I	alloy II	alloy I	alloy II
0.00	400	290	400	290	400	290	400	290
$1 \times 10^{-5}$	505	366	490	350	450	324	425	305
$5 \times 10^{-5}$	610	440	565	428	510	360	462	325
$1 \times 10^{-4}$	650	466	600	400	535	375	480	335
$5 \times 10^{-4}$	752	540	685	485	575	410	512	355
$1 \times 10^{-3}$	800	575	720	510	605	421	525	365

Figs. 10 and 11 show the variation of galvanic current with time for alloys I and II, respectively, immersed in different concentrations of NaCl (0.01-1 M). The obtained plots indicate that the galvanic current of the alloy in NaCl solution firstly decreases reaching a steady state and then, after an induction period of time, the galvanic current abruptly rises. This sudden rise in galvanic current is an indication of the occurrence of pitting corrosion on the surface of the alloys immersed in NaCl solution.

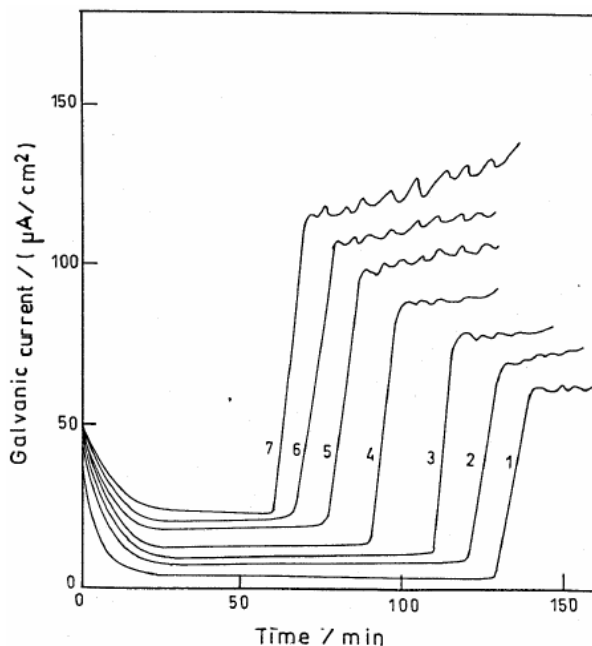


**Figure 10.** Galvanic current-time curves for alloy (I) in NaCl solutions of different concentrations: 1- 0.01, 2- 0.05, 3- 0.1, 4- 0.25, 5- 0.5, 6- 0.75, 7- 1.0 M.

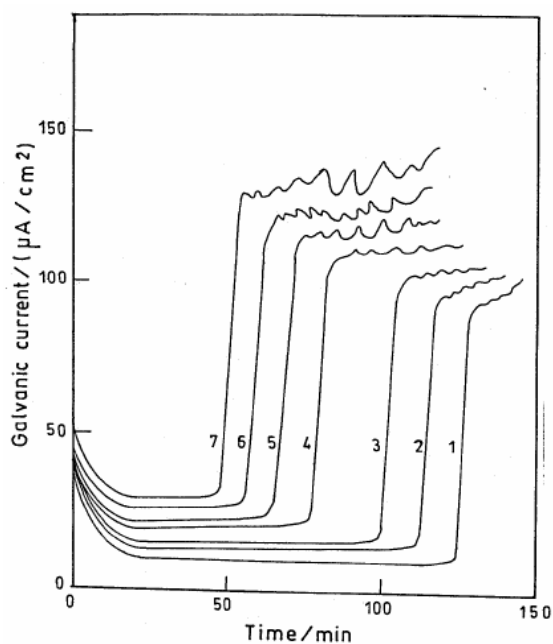


**Figure 11.** Galvanic current-time curves for alloy (II) in NaCl solutions of different concentrations: 1- 0.01, 2- 0.05, 3- 0.1, 4- 0.25, 5- 0.5, 6- 0.75, 7- 1.0 M.

The dependence of induction period on the chloride ion concentration is shown in Fig. 12. This figure represents the variation of the induction period with the logarithm of the molar concentration of the chloride ions for the alloys I and II.

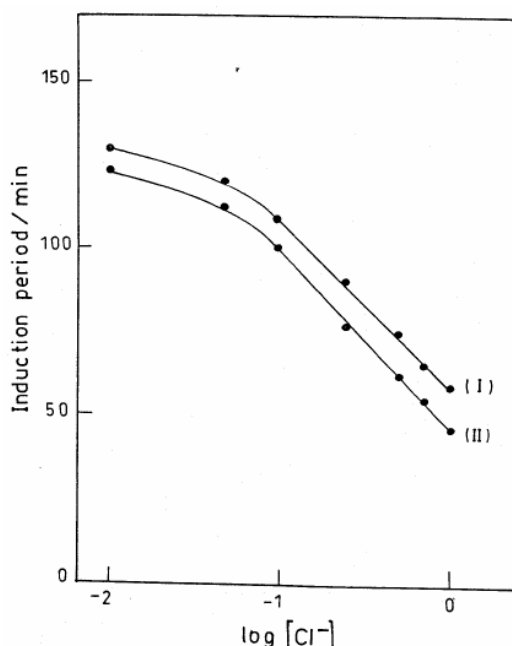


**Figure 12.** Dependence of induction period on the logarithm of chloride ion concentration for alloys (I, II).

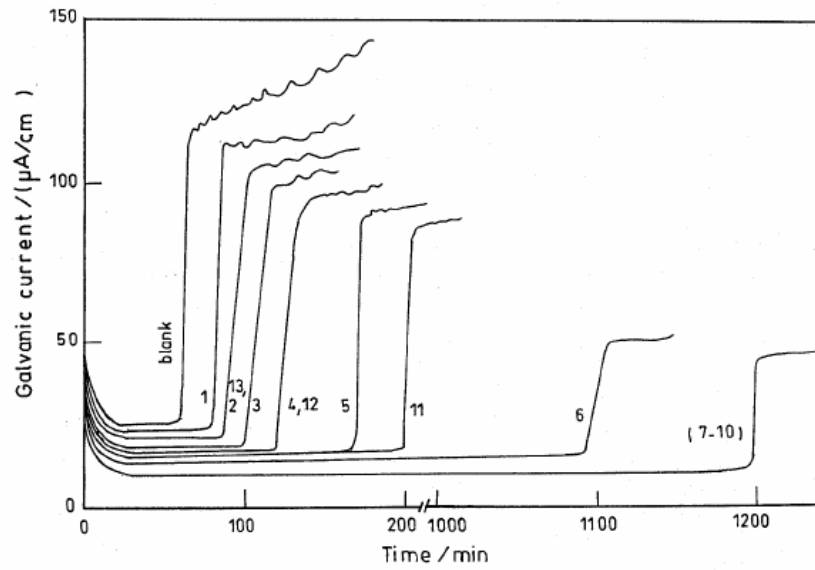
The general features of the plots of this figure are the same as that of plots of Fig. 3 ( $E_{\text{pit}}$  vs.  $C_{\text{Cl}^-}$ ). This gives a chance to assume the empirical relationship between the induction period and the logarithm of the chloride ions concentration in the form:

$$t_{\text{ind}} = a_3 - b_3 \log C_{\text{Cl}^-} \quad (3)$$

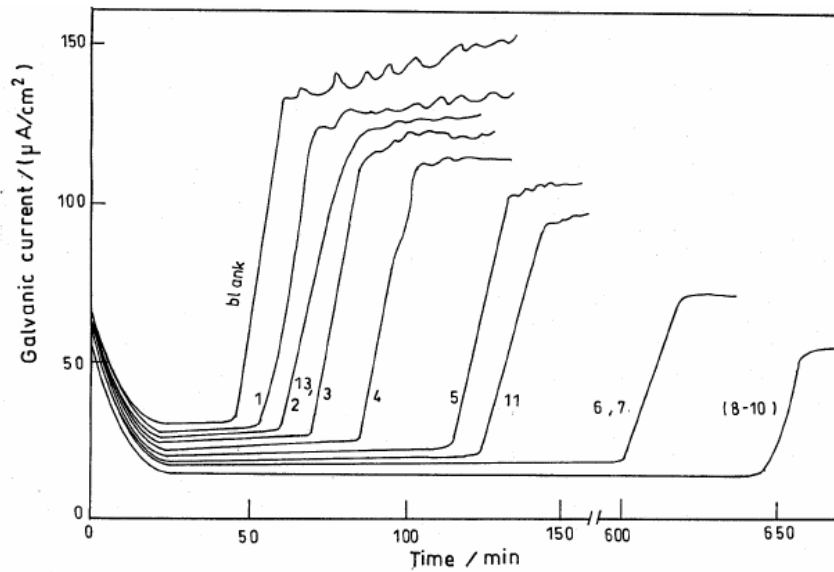
where  $a_3$  and  $b_3$  are constants, which depend on the nature of the metal and type of the aggressive anion. However, in the case under consideration, the plot of the two variables (Fig. 12) gives rise to curves of sigmoidal nature in which equation (3) is obeyed only within a limited range of chloride ions concentrations. The value of  $b_3$  is deduced from the plots of Fig. 12 and is found to be 50 and 55 min/decade for alloys I and II, respectively. This indicates that alloy II is more susceptible to pitting corrosion in NaCl solutions than alloy I. This conclusion firms the results obtained by the potentiodynamic anodic polarization measurements.

Figs. 13 and 14 represent the variation of galvanic current with time for alloys I and II, respectively, in 1.0 M NaCl containing  $10^{-3}$  M of each of the organic additives (1-13). Inspection of the plots of these figures reveals that the galvanic current of the alloy firstly decreases with reaching state and after an induction period the current increases suddenly and markedly, indicating the occurrence of pitting corrosion on the surface of the alloys. The induction period is deduced

from the plots of Figs. 13 and 14 and it is listed in Table 6 for alloys I and II, respectively.



**Figure 13.** Galvanic current-time curves for alloy (I) in 1.0 M NaCl solution containing  $10^{-3}$  M of compounds (1-13).

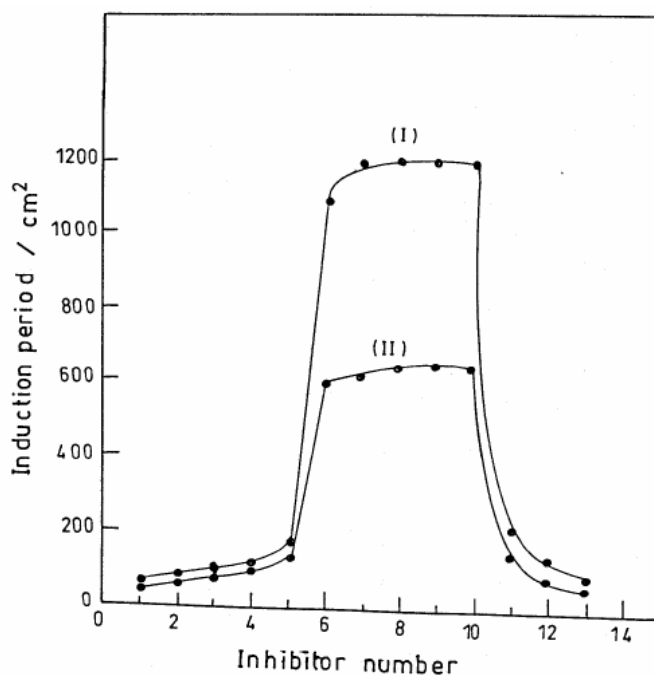


**Figure 14.** Galvanic current-time curves for alloy (II) in 1.0 M NaCl solution containing  $10^{-3}$  M of compounds (1-13).

The magnitude of the induction period greatly depends on the type of both alloy and organic additives, as shown from the plots of Fig. 15. It is indicated from these plots that the magnitude of the induction period gradually increases from compounds (1-5) and then abruptly rises and remains high up to compound (10).

**Table 6.** Data of galvanic current-time measurements for alloys I and II in 1.0 M NaCl solution containing  $10^{-3}$  M of organic additives.

Solution	alloy I		alloy II	
	Induction period / min	Inhibition efficiency I%	Induction period / min	Inhibition efficiency I%
blank	60	—	45	—
1	80	20	53	15
2	86	30	60	25
3	100	40	70	35
4	120	50	80	45
5	170	65	113	60
6	1090	94.5	600	92.5
7	1200	95	600	92.5
8	1200	95	643	93
9	1200	95	643	93
10	1200	95	643	93
11	200	70	129	65
12	120	50	82	45
13	86	30	60	25

**Figure 15.** Induction period for alloys (I, II) in 1.0 M NaCl solutions containing  $10^{-3}$  M of compounds (1-13).

After this the induction period greatly decreases for the compounds (11-13). In all cases, the presence of the organic additive in NaCl solution increases the magnitude of the induction period, indicating that these organic additives have an inhibiting effect on the pitting corrosion of the alloy in NaCl solution. If we roughly assume that the magnitude of the induction period is directly

proportional to the inhibition efficiency of the additive thus, the inhibition efficiency,  $I\%$ , of the compound can be calculated from the relationship:

$$I\% = \left(1 - \frac{t_{ind,free}}{t_{ind,inh}}\right) \times 100$$

where  $t_{ind,free}$  and  $t_{ind,inh}$  are the induction periods in absence and in presence of the organic additive, respectively. The calculated values of inhibition efficiency of the organic additive for the pitting corrosion of alloys I and II are listed in Table 6, and depicted in Fig. 16. The general features of the plots of this figure are the same as those of plots of Figs. 8, 9 and 15. From the data of Table 6 and Fig. 16 it can be seen that the inhibition efficiency,  $I\%$ , of the organic additives changes according to the order:  $1 < 2 < 3 < 4 < 5 \ll 6 \cong 7 \cong 8 \cong 9 \cong 10 \gg 11 > 12 > 13$ . This order is the same as that obtained from the potentiodynamic anodic polarization measurements.

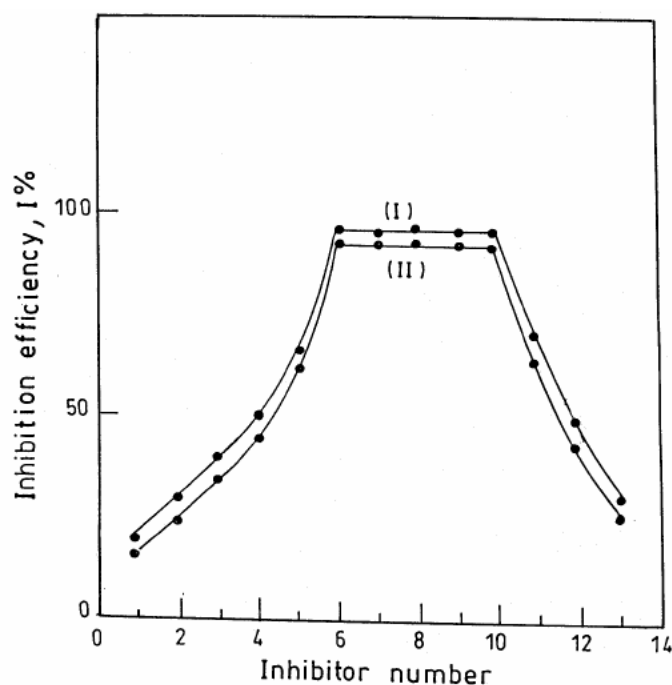


**Figure 16.** Inhibition efficiency for alloys (I, II) in 1.0 M NaCl solutions containing  $10^{-3}$  M of compounds (1-13).

The obtained results indicated that alloy II is more susceptible to corrosion than alloy I. This may be due to difference in chemical composition of the two alloys, where alloy (I) contains (Cu + Fe) and alloy (II) contains (Cu + Al + Fe). The presence of aluminium in alloy II leads to the formation of heterogeneous phases which have different potentials. The phases of  $\text{CuAl}_2$  and  $\text{FeAl}_3$  may precipitate at the grain boundaries, where these phases are cathodic to the matrix. This state favors the localized attack of the aggressive ions (such as Cl). The passivation of alloy I occurs on the account of the formation of iron oxides, copper oxides and copper oxychlorides. In the case of alloy II the passivation occurs on the account of the formation of iron oxides, copper oxides and copper oxychlorides and also aluminium oxide. If activating agents, such as chloride ions, are present in the

electrolyte, then the passive state is disturbed and the process of dissolution is accelerated. This is because chloride ions displace water molecules by virtue of their negative charge and their adsorption on the metal surface. Also, since the coating of the surface with oxygen is non-uniform, in places where there are defects in the structure of the oxide film, it will start predominantly the adsorption of chloride ions. Thus in addition to the passivating oxides and oxychlorides, a halide possessing good solubility will be formed and the dissolution is accelerated by means of setting up of the pitting corrosion [7]. This type of corrosion can be suppressed with the aid of anions or molecules (as additives) which are able to prevent adsorption of chloride ions or to dislodge them from the metal surface. In this electrolyte, it would imply that here the role is played by a concurrent adsorption of halide ions and passivating and / or inhibiting species. For higher concentration of passivating and / or inhibiting species the adsorption of aggressive ions (such as chloride ions) can be excluded completely.

As comes evident from the data of the effect of organic additives (monocarboxylates  $C_nH_{2n+1}COO^-$ ,  $n=1-13$ ), short chain length ( $n \leq 5$ ) monocarboxylates were mild inhibitors for the pitting corrosion of the tested alloys I and II. However, at  $n = 6$  inhibitor effectiveness rose abruptly and remained high up to  $n = 10$ . This level of inhibition decreased in an equally dramatic manner at  $n = 11$  and declined further up to  $n = 13$ . It was assumed that the inhibition of pitting corrosion just took place by the formation of a protective film on the alloys surface which acted as a physical barrier against aggressive species [16].

Although the carboxylic acids are weak, at  $pH \cong 8.4$  they will be present almost entirely in their anionic form. Furthermore, as their  $pK_a$  values vary weakly with chain length (4.75 - 4.92) [10], the greatly enhanced inhibition at  $6 \leq n \leq 10$  could not be due to changes in inhibitor speciation or to enhanced surface complexation. The most likely explanation was enhanced surface adsorption at the hydrated metal oxide/hydroxide surface due to the increasing hydrophobicity of the carboxylate anions with increasing chain length.

The equally abrupt decline inhibitor efficiency at  $n = 11$  was almost certainly due to a decrease in solubility and / or increasing micellization of the carboxylate anions in the test solutions, leading to decreased surface coverage via adsorption of carboxylates on the alloys surface [10]. In addition, we may account to the steric hindrance and / or change of the mode of adsorption on the electrode surface.

The behaviour observed for the monocarboxylates contrasted with that reported for surfactant-type inhibitors such as substituted aminocarboxylic or sulphonic acids, where inhibition of mild steel corrosion could be achieved only at inhibitor concentration greater than the cmc [17]. Similarly, good inhibition of carbon-steel corrosion by monoalkylphosphonate [18] and of iron corrosion by 1-decylimidazole [19], both in 3 % NaCl solution, occurred only at concentrations greater than the cmc.

The present data clearly indicated that there is an optimal chain length for effective inhibition of alloys pitting corrosion in saline, near-neutral solutions by saturated straight chain monocarboxylates. There is no advantage and possibly

serious disadvantage in using longer chain length carboxylates per se. In this connection, the present optimal chain length ( $6 \leq n \leq 10$ ).

It has been shown that inhibitive properties of monocarboxylates toward alloys I and II pitting corrosion in neutral, saline solutions are largely dependent on their affinity for the adsorption sites on the metal oxide, oxychloride, hydride surface and their ability to displace  $\text{Cl}^-$  ions [20]. The moderate change of  $E_{\text{pit}}$  and induction period to carbon length for  $n < 6$  indicated that this affinity changed moderately for these species. At longer chain lengths ( $n \geq 6$ ), the hydrophobicity of the hydrocarbon “tails” has been suggested to become the predominant factor [21].

There was the possibility that for long chain monocarboxylates, adsorption might be enhanced by the creation of a second layer of inhibitor via the lipophilic interaction of the hydrocarbon tails leading to a hemimicelle or bilayer, as shown in Fig. 17. The formation of such hemimicelles (bilayer) has been reported in many studies [17,18,21-24].

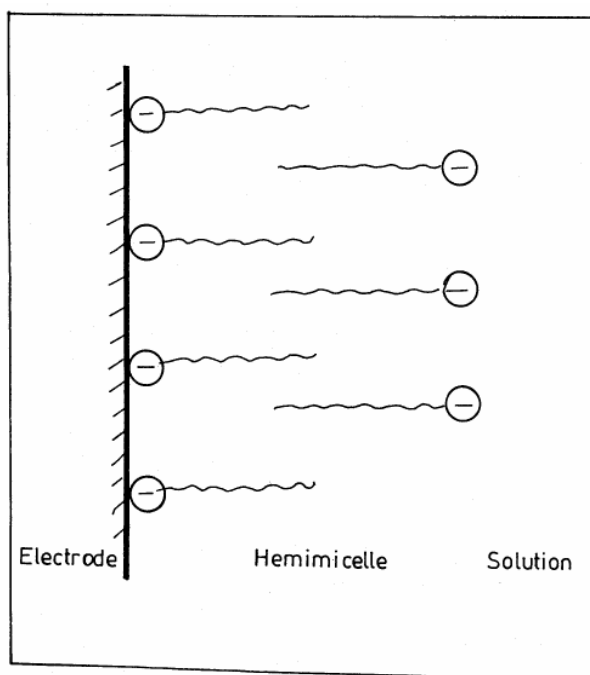


**Figure 17.** Formation of a hemimicelle layer on electrode surface.

It is possible that the formation of such bilayers has been responsible for the sudden rise in  $I\%$  observed for monocarboxylates with alloys I and II. From the standpoint of pitting inhibition [20], the need of  $\text{Cl}^-$  to averse two negatively charged sheets and hydrophobic layer of considerable thickness might explain the exceptional inhibiting properties of the higer monocarboxylates for very long chain length monocarboxylates ( $n=11, 12, 13$ ).

## Conclusions

From the obtained results, the following conclusions can be drawn:

1. The pitting corrosion susceptibility of the tested alloys I and II increases with the increase of chloride ion concentration.

2. Alloy II is more susceptible to pitting corrosion than alloy I, which may be attributed to the difference in the chemical composition of the two alloys and the presence of aluminium in alloy II.
3. Straight chain aliphatic monocarboxylates ( $C_nH_{2n+1}COO^-$ ,  $n=1-13$ ) can be excellent inhibitors for pitting corrosion of the tested alloys in aerated, saline, near neutral aqueous solution, but their effectiveness is critically dependent on their chain length. The range of chain lengths producing optimal inhibition was ( $6 \leq n \leq 10$ ).
4. For the monocarboxylates, it appeared to be no general advantage in using long chain length species.
5. The complex dependence of I % on straight chain aliphatic carboxylates appeared to be reflection of competing reactions involving adsorption at metal oxide / hydroxide surface and solubility and micelle formation in the solution.
6. There is a great agreement between the results obtained by potentiodynamic anodic polarization and galvanic current measurements.

## References

1. C.C. Nathan, ed., "Corrosion Inhibitors" (Houston, TX : NACE, 1973).
2. M.W. Ranney, Corrosion Inhibitors: Manufacture and Technology [Park Ridge, NJ: Noyers Data Corp., 1976].
3. M.J. Collic, ed., Corrosion Inhibitors: Development Since 1980 [Park Ridge, NJ: Noyers Data Corp. 1983].
4. H.H. Uhlig, R.W. Revie, Corrosion and Corrosion Control: An Introduction to Corrosion Science and Engineering (New York, NY: John Wiley and Sons 1985).
5. S. Turgoose, "Mechanism of Corrosion Inhibition in Neutral Environments", in Chemical Inhibitors for Corrosion Control, ed., B.G. Clubley [Cambridge, U. K: Royal Society of Chemistry, 1990].
6. R.B. Beal, ed., Engine Coolant Testing: Second Symp. ASTM STP (887 Philadelphia, PA: ASTM, 1986).
7. I.L. Renzfeld, Corrosion Inhibitors [New York, NY: McGraw-Hill, 1981].
8. G. Trabanelli, In Corrosion Mechanisms, ed., F. Mansfeld [New York, NY: Marcel Dekker, 1987].
9. A.D. Mercer, 7<sup>th</sup> Europ. Symp. Corrosion Inhibitors [Ferrara, Italy, Univ. Ferrara, 1990].
10. G.T. Helter, N.A. North, S.H. Tan, *Corrosion* 53-8 (1997) 657.
11. Z.A. Foroulis, M.J. Thubrik, *Werkstoffe und Korros.* 25 (1975) 350.
12. H.C. Brookes, F.J. Graham, *Corros. Sci.* 45-4 (1989) 278.
13. M. Abdallah, S.M. Abdelhaleem, *Bull. Electrochem.* 12 (1996) 449.
14. S.M. Abdelhaleem, *Werkstoffe und Korros.* 30 (1979) 631.
15. S.M. Abdelhaleem, *Brit. Corros. J.* 14 (1979) 171.
16. W. Qafsaoui, Ch. Blanc, J. Roques, N. Pebere, A. Srhiri, C. Mijoule, G. Mankowski, *J. Appl. Electrochem.* 31 (2001) 223.
17. A. Weisstuch, K.R. Lang, *Mp.* 10 (1971) 29.

18. M. Dupart, A. Shiri, Y. Derbali, N. Pebere, *Electrochemical Methods in Corrosion Research*, vol. 8, ed. M. Dupart (Zurich, Switzerland *Trans. Tech. Publications* (1986) 267.
19. N. Pebere, M.C. Lafont, A. Savignac, F. Dabosi, 7<sup>th</sup> Europ. Symp. Corrosion Inhibitors (Ferrara, Italy, Uni. Ferrara, 1990, p. 1353).
20. B.W. Samuels, K. Sotoudeh, R.T. Foley, *Corrosion* 37 (1981) 92.
21. H. Ulrich, W. Stumm, *Environ. Sci. Technol.* 22 (1988) 37.
22. I.M. Abrantes, I.M. Castillo, C. Norman, I.M. Peter, *J. Electroanal. Chem.* 163 (1984) 209.
23. D.W. DeBerry, A. Viehbeck, *J. Electrochem. Soc.* 133 (1986) 30.
24. D.W. DeBerry, A. Viehbeck, *Corrosion* 44 (1988) 299.